JOURNAL OF MAGNETIC RESONANCE 78, 440–458 (1988)

Variable-Rate Selective Excitation

STEVEN CONOLLY, DWIGHT NISHIMURA, AND ALBERT MACOVSKI

Magnetic Resonance Systems Research Laboratory, Stanford University, Stanford, California 94305

AND

GARY GLOVER

General Electric Medical Systems Division

Received July 6, 1987; revised December 10, 1987

A procedure is introduced for refabricating any spatially selective excitation pulse to reduce its SAR while preserving its duration and slice profile. Called variable-rate selective excitation, the procedure allows for a variable trade-off of RF amplitude for duration at each sample of the pulse. SAR reduction of 50% is possible with only a mild smearing of the off-resonance slice profile. Experimental slice profiles verify the principle. © 1988 Academic Press, Inc.

INTRODUCTION

The specific absorption rate (SAR) of a selective radiofrequency pulse is a critical parameter in a clinical setting. FDA SAR limitations restrict the minimum scan time for a given pulse sequence. The relatively high SAR of some new and otherwise desirable RF pulses may limit their clinical use. Moreover, RF amplifier hardware limitations may preclude the use of high SAR pulses.

Although there has been a great deal of effort toward selective pulse design in the past decade, very little has been done to ameliorate the SAR of a given pulse. In fact, many of the numerical design techniques introduced recently produce relatively high SAR pulses. For example, the optimal control approach (*1, 2*) computes RF pulses that deliver remarkably rectangular slice profiles but deposit a relatively large amount of power. Murdoch (*3*) reports that incorporating RF inhomogeneity robustness into the optimal control algorithm exacerbates the SAR problem even further. The hyperbolic secant pulse of Silver *et al.* (*4*), which inverts a slice even in the presence of substantial RF inhomogeneity, has even higher SAR.

Coer-Joly reports (*5*) that pulse-width modulation can deliver sharp selective excitation profiles and noted that the SAR and peak magnitude of his selective excitation pulses were far less than conventional amplitude-modulated pulses. The essence of SAR reduction is clear from this effort: one needs to distribute the pulse amplitude uniformly over the excitation interval. Pulse-width (PW) modulation is not as flexible as one would like. First, hardware changes are required. Second, the pulses designed in the literature for AM and FM transceivers cannot be incorporated. Finally, PW

0022-2364/88 $3.00

modulation forces an inherent trade-off between the number of parameters available for pulse design and the pulse duration. This is not the case for AM and FM pulses.

In this paper we do not discuss a pulse design technique. Instead we introduce a new technique for pulse *refabrication.* That is, we propose an algorithm that takes a previously designed RF pulse and computes a new pulse and a new (time-varying) slice-select gradient waveform. The new pulse performs the selective excitation exactly as the original pulse, but at significantly lower SAR and peak amplitude. In a sense, we have added a degree of freedom to the PW modulation scheme, namely, the time variation of the gradient waveform.

The new pulse refabrication scheme is called *v*ariable-*r*ate *s*elective *e*xcitation, abbreviated VERSE. The algorithm is based on the fundamental Larmor relation: a magnetization vector will precess at a frequency determined by the strength of the local magnetic field. During one sample of a selective excitation pulse, the field is determined by the gradient and RF fields. It is obvious that only the net rotation is critical rather than the rate of rotation. Hence, one can perform an identical excitation twice as long with half the field strength. The key innovation is to allow this trade-off of time and amplitude to *vary* at each sample in the pulse. Since most RF pulses are very peaked at the middle, one should flatten the amplitude in the middle and extend the duration of each of its samples, while expediting and, hence, amplifying the side lobes. It is this uniform redistribution of the pulse area that affords the decrease in SAR.

We first derive the principle of VERSE, then detail some algorithms that exploit the principle for SAR reduction. Off-resonance effects are discussed and implementation details are addressed. Experimental results are presented for each algorithm.

THE VERSE PRINCIPLE

The fundamental Larmor relation,

$$\omega = \gamma \|\mathbf{B}\|,$$

gives the precession frequency of a magnetization vector in the presence of an external magnetic induction field, **B**. During one sample of duration Δt, from a piecewise-constant RF pulse, a magnetization vector precesses an angle $\theta = \omega \Delta t$. One could achieve the same angle of precession by exciting the spins for twice as long with a parallel induction field half as strong, because the precession angle is the product of the frequency and duration. This basic fact is depicted in Fig. 1. Note that each time sample is independent of the other samples; there is no constraint to reduce each of the RF pulse samples equally. Because each of the individual angles of precession is unchanged, the product of the rotations will not change, and the selective excitation profile will not be altered. This is the fundamental principle of variable-rate selective excitation.

The mathematical equivalent of the heuristic explanation above relies on the Bloch equation, which describes the spin mechanics during selective excitation. Let $B_1(k) = B_I(k) + iB_Q(k)$ represent samples from a piecewise constant complex RF pulse. That is, the RF has amplitude $B_1(k)$ from time $(k-1)\Delta t$ to $k\Delta t$. Let G be the z-gradient amplitude during the selective excitation. Assuming that relaxation is negligible during

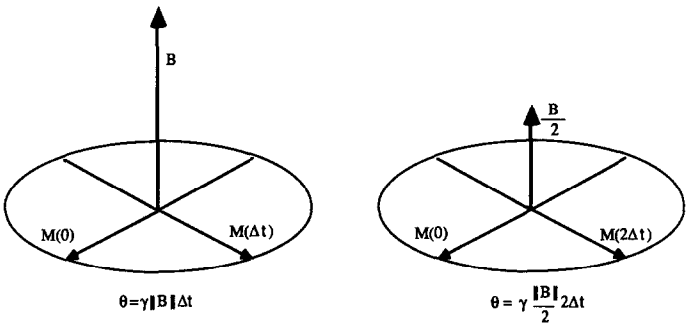

FIG. 1. The same rotation can be accomplished at different speeds.

the pulse, the magnetization vector at time $T = N\Delta t$ is the ordered product of rotation matrices multiplied by the initial magnetization distribution (*6*):

$$\mathbf{M}(z, T) = \prod_{k=N}^{1} \exp\left(\begin{bmatrix} 0 & Gz & -B_Q(k) \\ -Gz & 0 & B_I(k) \\ B_Q(k) & -B_I(k) & 0 \end{bmatrix} \gamma \Delta t\right) \mathbf{M}(z, 0).$$

Define an excitation amplitude-reduction factor $\alpha(k)$. Note that if the kth sample is applied for a duration $\Delta t/\alpha(k)$, and if all of the excitation fields are multiplied by the same factor $\alpha(k)$, then the kth rotation matrix will be unchanged:

$$\exp\left(\begin{bmatrix} 0 & \alpha(k)Gz & -\alpha(k)B_Q(k) \\ -\alpha(k)Gz & 0 & \alpha(k)B_I(k) \\ \alpha(k)B_Q(k) & -\alpha(k)B_I(k) & 0 \end{bmatrix} \frac{\gamma \Delta t}{\alpha(k)}\right).$$

Comparison of the rotation matrices leads one to conclude that an excitation of duration $\Delta t/\alpha(k)$ and with a new RF pulse $\alpha(k)B_1(k)$ and a new time-varying gradient waveform $\alpha(k)G$ will elicit the same slice profile as the original pulse at uniform rate. The $\alpha(k)$ represent a degree of freedom previously unexploited.

It is convenient to name this new set of pulse variables. Let $b_1(k) = \alpha(k)B_1(k)$ and let $g(k) = \alpha(k)G$. These are the VERSE excitation waveforms. We will call them *facsimile pulses,* since they perform the same function as the original pulse and gradient. Finally, define $t(k) = \Delta t/\alpha(k)$. Recall that the new excitation waveforms must be parallel and each has the same area as the original pulse. These facsimile conditions are summarized below:

$$\begin{bmatrix} b_I(k) \\ b_Q(k) \\ g(k) \end{bmatrix} t(k) = \begin{bmatrix} B_I(k) \\ B_Q(k) \\ G \end{bmatrix} \Delta t.$$

SAR REDUCTION

We now demonstrate that VERSE can reduce the SAR for a given RF pulse. First, only two rates are employed. Figure 2 shows a sinc pulse and its uniform-rate gradient. Figure 3 shows a two-speed facsimile RF and gradient pulse pair. Note that the middle

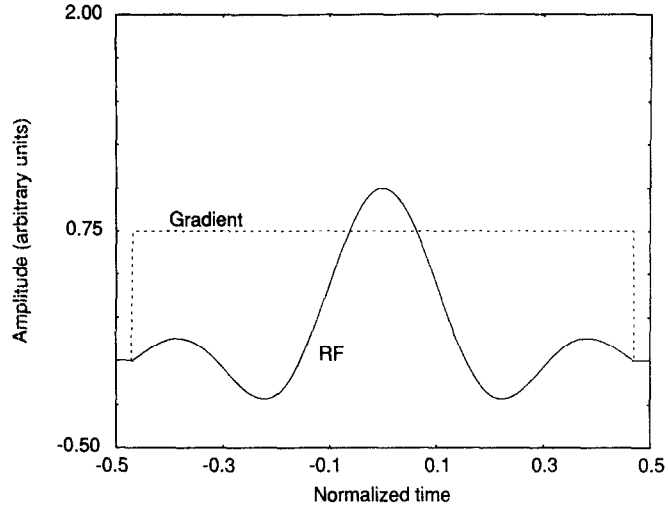

FIG. 2. Uniform-rate sinc pulse and gradient.

of the pulse has been slowed down and attenuated. The side lobes have been accelerated and amplified so that the overall duration of the pulse is unchanged. It should be clear that the VERSE pulse has lower SAR than the original sinc pulse. Of course, this is not a practical example since slew-rate limitations would preclude the use of this particular gradient waveform.

The SAR formulas derived in this section will be used extensively in the following section. For ease of comparison, we consider only equal-duration facsimile pulses. Hence, we are concerned with the energy in a particular pulse, rather than its average

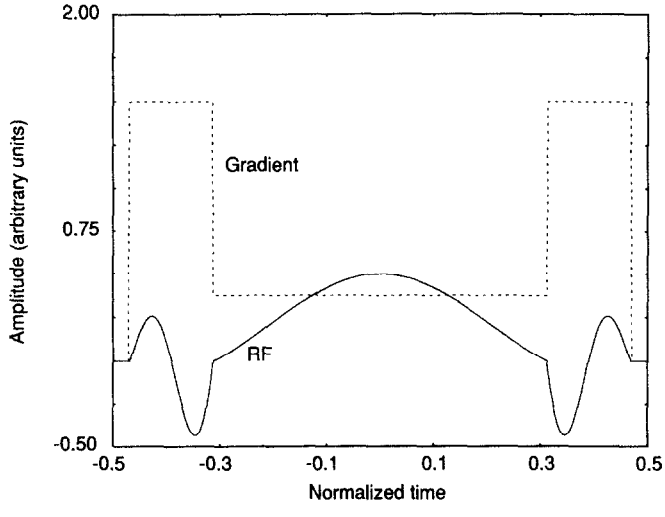

FIG. 3. Two-speed VERSE RF and gradient pulses.

power, which differs only by a constant factor. The energy delivered during a pulse is proportional to the integral of squared magnitude of the RF. Hence,

$$\text{SAR} \propto \int_0^T |b_1(t)|^2 dt. \quad [1]$$

For a piecewise constant variable-rate RF pulse,

$$\text{SAR} \propto \sum_{k=1}^{N} |b_1(k)|^2 t(k). \quad [2]$$

Because the variables must satisfy the facsimile conditions, the SAR equation can be cast as a function of one waveform, which we can pick at our convenience. Moreover, knowledge of any one of the VERSE waveforms provides complete information for computation of the remaining VERSE waveforms. Using the facsimile conditions one can show that

$$\text{SAR}(\mathbf{t}) \propto \sum_{k=1}^{N} \frac{|B_1(k)|^2}{t(k)}, \quad [3]$$

and

$$\text{SAR}(\mathbf{g}) \propto \sum_{k=1}^{N} |B_1(k)|^2 g(k), \quad [4]$$

where $|B_1(k)|^2$ is defined to be squared magnitude of the original pulse, $B_I^2(k) + B_Q^2(k)$. We have also used the symbols **g** and **t** to describe the vectors with elements $g(k)$ and $t(k)$.

SAR-REDUCED PULSES

There are several SAR-reduction formulations that have proven useful. We discuss three of the most promising here. We have chosen to abandon gradient slew-rate constraints in order to retain closed-form solutions. This is reasonable because the slew-rate constraint can be incorporated after the VERSE pulse is computed with only a mild SAR penalty. We discuss this gradient smoothing in the implementation section.

Minimum-SAR facsimile. In this formulation, we minimize the SAR subject to maximum gradient and constant duration constraints. The minimum-SAR optimization problem is

$$\min_{\mathbf{g}} \text{SAR}(\mathbf{g}) = \sum_{k=1}^{N} g(k)|B_1(k)|^2, \quad [5]$$

subject to

$$\sum_{k=1}^{N} t(k) = N\Delta t \quad [6]$$

$$g(k) < G_{\max}. \quad [7]$$

First, we cast the time constraint equation into gradient variables:

$$\sum_{k=1}^{N} \frac{1}{g(k)} = \frac{N}{G}. \quad [8]$$

In Appendix A, we show that the minimum-SAR RF pulse is indeed very close to a constant magnitude pulse. We show that unless the VERSE gradient violates the maximum gradient constraint, the RF has constant magnitude. If the maximum gradient constraint is violated at a particular index k, then the optimal (constrained) gradient at that index is G_{max}, and the new RF must be smaller in magnitude than the constant. Specifically, we derive the minimum-SAR gradient,

$$g(k) = \min\left\{G_{max}, \frac{c}{|B_1(k)|}\right\}. \quad [9]$$

One would hope that the time constraint would give a closed-form solution for the constant c. However, it admits only an iterative solution, as one does not know which of the $g(k)$ violates the G_{max} constraint until one has computed c. We use a simple algorithm to determine c. First, we assume that none of the gradient values exceeds G_{max}. Then we calculate $c^{(1)}$ from the time constraint, Eq. [8]:

$$\frac{1}{c^{(1)}} \sum_{k=1}^{N} |B_1(k)| = \frac{N}{G}. \quad [10]$$

Equation [9] allows us to then check which of the $g(k)$ violates the G_{max} constraint. We then adjust those $g(k)$ to G_{max} and again use the time constraint equation to calculate $c^{(2)}$. This is continued until no new constraint violations occur. Convergence is achieved in a few iterations.

Figure 4 shows to scale a uniform-rate optimal control selective 180° pulse designed for spin-echo generation in our lab (*2*) and its minimum-SAR facsimile. For all pulses

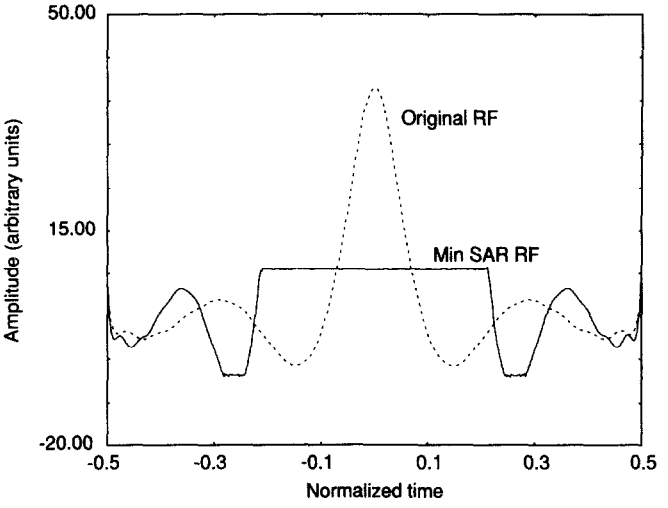

FIG. 4. Uniform-rate and VERSE minimum-SAR RF waveforms.

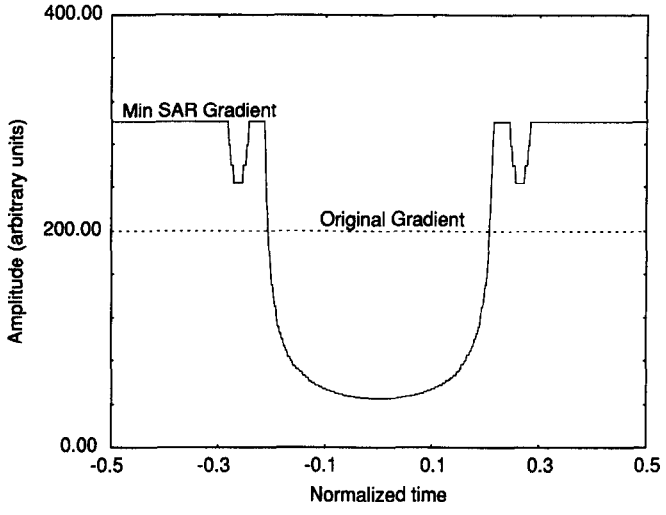

FIG. 5. Uniform-rate and VERSE minimum-SAR gradient waveforms.

designed in this paper, the ratio of G_{max}/G was set to 3/2. We must emphasize that lower ratios will afford less SAR reduction. Equivalently, pulse duration can be extended variably if one is constrained to $G_{max}/G = 1$, but the slice profile will invariably be thicker than the minimum possible.

Figure 5 shows the uniform-rate and VERSE gradient waveforms. Figure 6 is an experimental slice profile of the uniform-rate pulse obtained on a 1.5 T General Electric Signa system by reading out a spin echo in the slice-select direction. Only the 180° pulse was selective. Figure 7 shows the magnitude experimental slice profile for the VERSE minimum-SAR facsimile pulse. Figure 8 shows the phase from the experi-

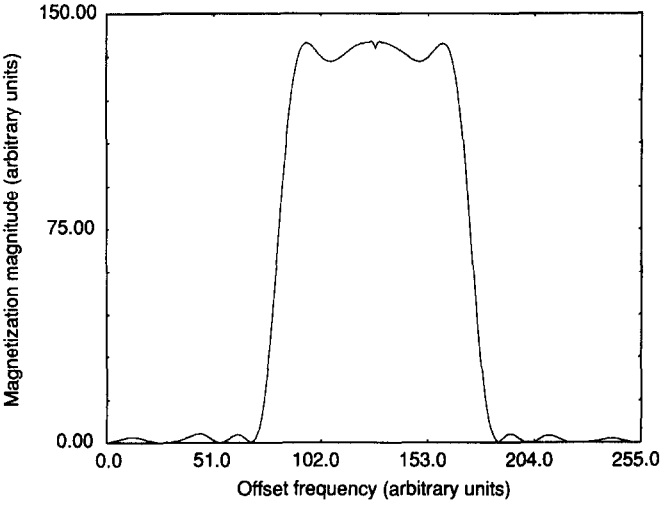

FIG. 6. Magnitude slice profile for uniform-rate 180° pulse.

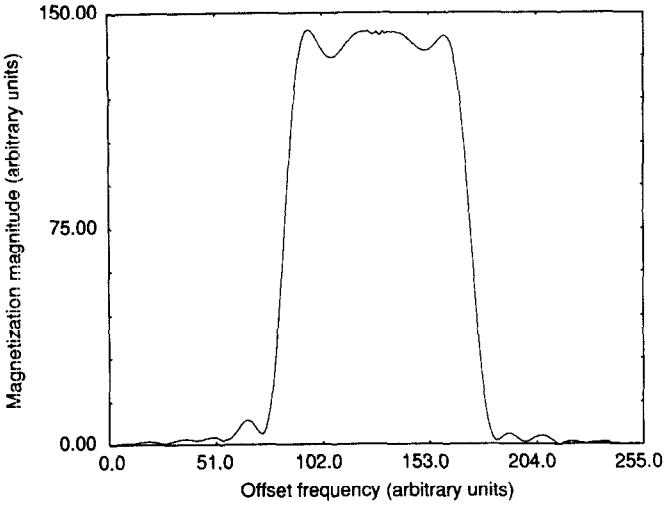

FIG. 7. Experimental minimum-SAR slice profile: magnitude.

mental data of Fig. 7. Note that the phase is linear in the slice-select direction and, hence, can be refocused with gradients. It is common to achieve 65% SAR reduction with this formulation. The SAR reduction depends on the particular pulse and the ratio G_{max}/G, with higher ratios improving the SAR reduction.

Peak-RF Constrained Facsimile. Often the peak-magnitude limitations on one's RF amplifier constrain the selective pulse one may use. For example, the peak amplitude of a fixed-duration sinc pulse increases linearly with the number of sinc side lobes. This is significant since the number of side lobes affects the quality of the slice

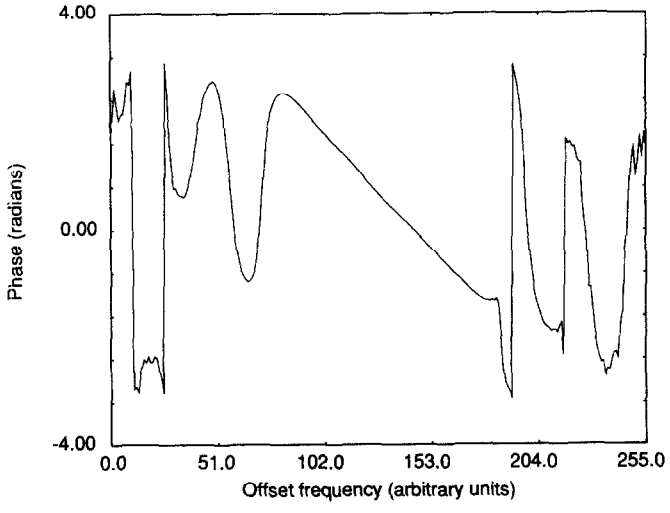

FIG. 8. Experimental minimum-SAR slice profile: phase.

profile. The minimum-time formulation addresses the peak-magnitude constrained problem. This formulation was explored in (*7*).

The minimum-time formulation is

$$\min_{t} \sum_{k=1}^{N} t(k), \qquad [11]$$

subject to gradient and peak-magnitude constraints:

$$|b_1(k)| < B_{max}, \qquad [12]$$

$$g(k) < G_{max}. \qquad [13]$$

Casting the constraints in the variable $t(k)$,

$$t(k) > \Delta t \frac{|B_1(k)|}{B_{max}}, \qquad [14]$$

$$t(k) > \Delta t \frac{G}{G_{max}}. \qquad [15]$$

The solution to this separable problem is obvious. To minimize the total duration, one should use the minimum $t(k)$ sufficient to satisfy the constraints. Hence,

$$t(k) = \Delta t \max\left\{\frac{G}{G_{max}}, \frac{|B_1(k)|}{B_{max}}\right\}. \qquad [16]$$

Figure 9 shows the minimum-time facsimile pulse for the uniform-rate 180° pulse shown in Fig. 4. The maximum RF value was set to roughly half the original peak value. Note that throughout the duration of the new pulse, either the gradient or the

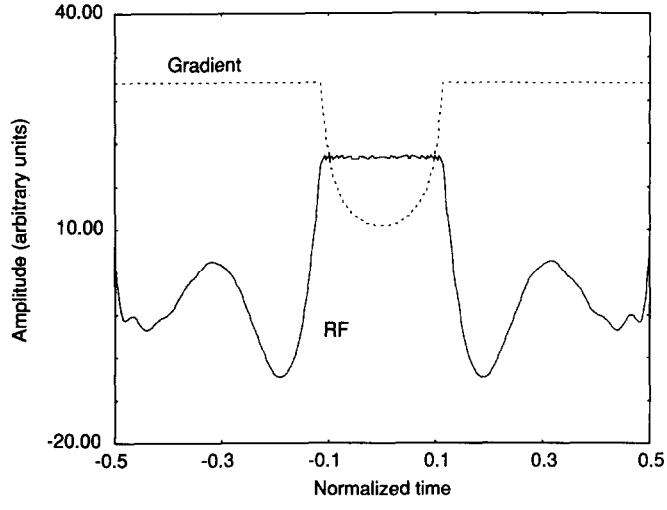

FIG. 9. Minimum-time facsimile of 180° pulse.

RF is at its maximum value. Figure 10 is the experimental slice profile for the minimum-time pulse.

Parametric optimization. Gradient slew-rate constraints were difficult to incorporate into the first two formulations. We now consider a parametric optimization that guarantees smooth gradient waveforms while minimizing SAR. We assume a parametric form for the gradient

$$g(k) = f(k, \mathbf{p}), \qquad [17]$$

where f is a smooth function of k, and $\mathbf{p}$ represents a parameter vector. The problem then consists of finding the optimal parameters $\mathbf{p}$. A time constraint is required; rewriting Eq. [6] in terms of the gradient,

$$\sum_{k=1}^{N} \frac{1}{g(k)} = \frac{N}{G}. \qquad [18]$$

To be explicit, the parametric optimization problem is

$$\min_{\mathbf{p}} \mathrm{SAR}(\mathbf{p}) = \sum_{k=1}^{N} f(k, \mathbf{p}) |B_1(k)|^2, \qquad [19]$$

subject to

$$\sum_{k=1}^{N} \frac{1}{f(k, \mathbf{p})} = \frac{N}{G}. \qquad [20]$$

The parameterization should be chosen so that both the maximum gradient amplitude and the maximum slew rate are intrinsically constrained. Furthermore, the number of parameters should be small. This formulation is amenable to numerical optimization.

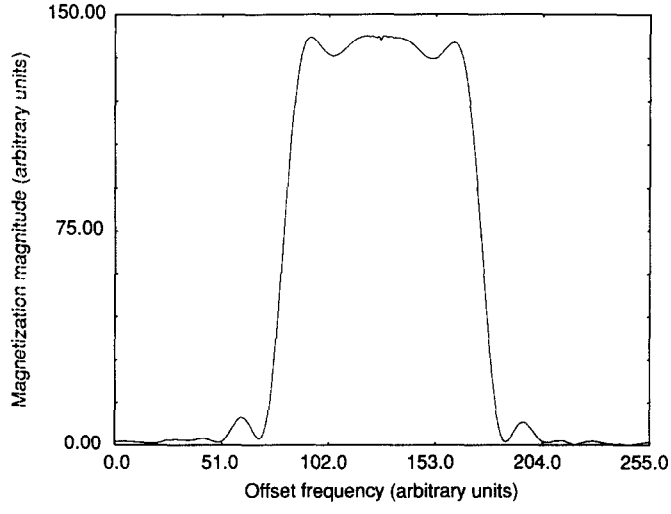

FIG. 10. Experimental slice profile for the minimum-time pulse.

Usually a simple plot of the SAR as a function of one free parameter is sufficient for optimization.

An example of parametric SAR minimization employs a Gaussian-shaped gradient waveform:

$$g(k) = G_{\max}[1 - ae^{-p(k-N/2)^2}]. \quad [21]$$

A simple algorithm for SAR minimization was developed. SAR was computed as a function of a on (0, 1). For each value of a, the corresponding value of p was computed to satisfy the time constraint. The VERSE pulse was then calculated using the optimal values of a and p.

We have used this technique (*8*) for SAR minimization of Silver's hyperbolic secant pulse (*4*). Figure 11 shows the original hyperbolic secant pulse, and Fig. 12 shows the VERSE minimum-SAR facsimile pulse shown on the same scale. The two gradient waveforms are plotted in Fig. 13. The minimum-SAR facsimile pulse has 43% of the SAR of the original pulse. The VERSE experimental inversion slice profile is shown in Fig. 14. The profile was obtained by reading out a spin echo in the slice-select direction following an inversion pulse. The slice width of the selective 90° pulse extends beyond the boundaries of the figure. Note that the duration of the VERSE pulse is identical to the original, and that the new pulse retains the original hyperbolic secant's remarkable insensitivity to RF inhomogeneity.

OFF-RESONANCE EFFECTS

Offset slices. Offset slices are essential for multislice imaging. It is well known that a modulated RF pulse produces a slice offset in proportion to the modulation frequency. Fortunately, there is an analogous technique for offsetting slices in the variable-rate framework. Instead of modulating with $\exp\{iz_0\gamma G(T - t)\}$ to offset a slice by z_0, one

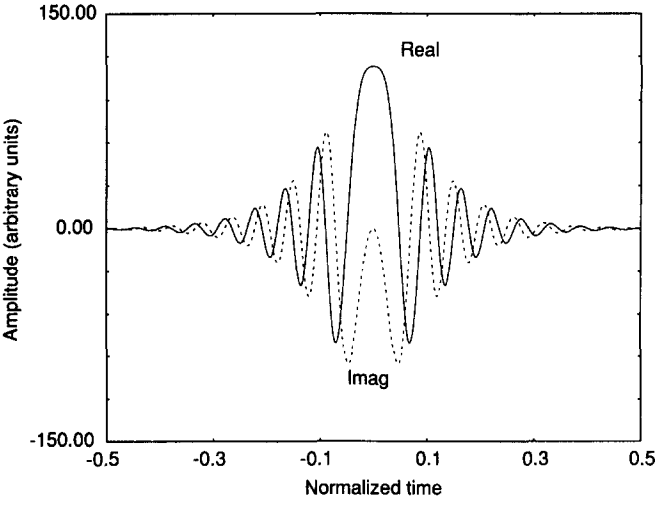

FIG. 11. Hyperbolic secant complex pulse.

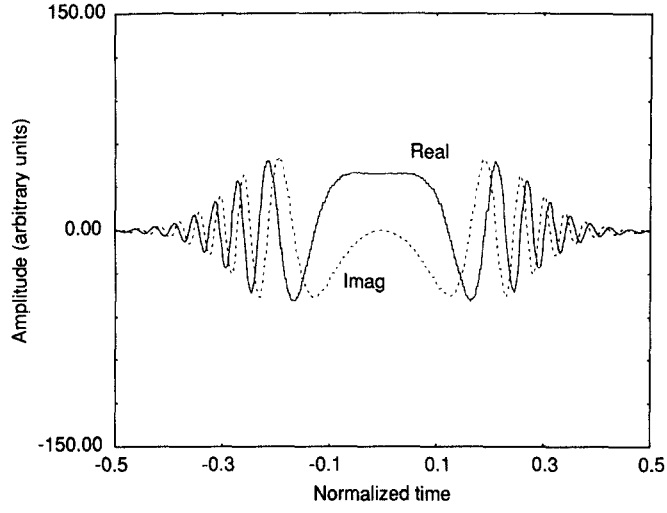

FIG. 12. VERSE RF facsimile of the hyperbolic secant.

needs to modulate with $\exp\{iz_0\gamma \int_t^T g(\tau)d\tau\}$. A proof of the shift theorem is included in Appendix B.

SHIFT THEOREM. *If a pulse,* $b_1(t)$, *and gradient,* $g(t)$, *excite a slice* $\mathbf{M}(z, T)$, *then* $b_1(t)\exp\{iz_0\gamma \int_t^T g(\tau)d\tau\}$ *and the same gradient excite the slice* $\mathbf{M}(z - z_0, T)$.

Chemical-shift effects. B_0 inhomogeneity and chemical-shift variations in the patient have significant effects on slice characteristics for any excitation scheme. With uniform-rate excitation, it is well known that a shift in the local field causes a shift in the slice profile. The superposition of such shifts in the receiving coil appears as a convolution

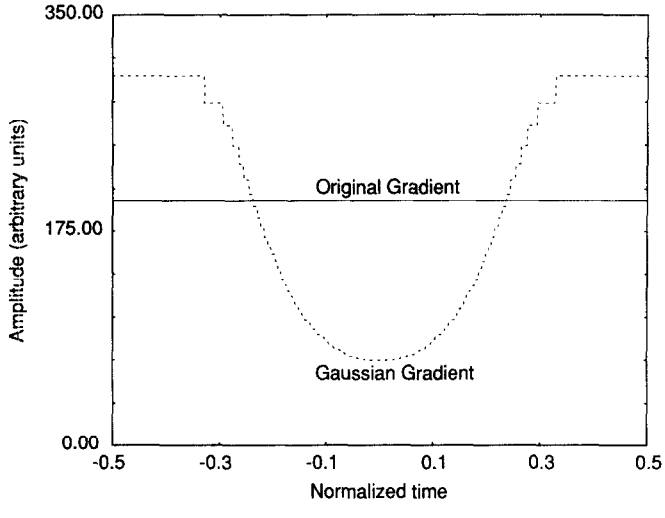

FIG. 13. Original and VERSE gradient waveforms.

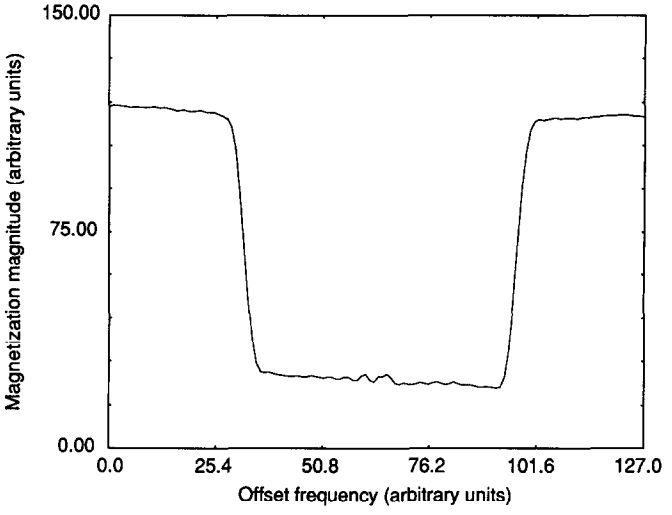

FIG. 14. Experimental inversion slice profile obtained with VERSE pulse.

of the slice profile with the inhomogeneity distribution. In this section we demonstrate the effect of chemical shift on the slice profiles generated by variable-rate pulses. This effect will be studied in greater depth in a future paper.

During uniform selective excitation in the presence of an offset frequency $\Delta\omega$, the z component of the excitation field is $\Delta\omega + \gamma Gz$. Hence, the slice is offset in position by $(\Delta\omega)/(\gamma G)$. During variable-rate selective excitation, the kth sample has z component $\Delta\omega + \gamma g(k)z$. Hence, the kth contribution from the piecewise constant RF is offset in position by $(\Delta\omega)/(\gamma g(k))$. Because this offset varies, the slice profile is smeared as well as shifted. Note that the offset is further the weaker the gradient. This is significant since most RF pulses are peaked at the center, requiring that the facsimile gradient pulse be very weak at the center. This means that the contributions to the slice profile from the key central portions of the RF will be spatially offset the most. From this perspective, it should be clear that the larger one "dips" into the gradient, then the worse is the off-resonance slice smearing. Of course, with no dip in the gradient, one sees only the shift effect.

To supplement this discussion, we include simulation results at a resonance offset frequency of 200 Hz. At 1.5 T, this is roughly the chemical shift between water and fat. Figures 15 and 16 show the gradient waveforms and the off-resonance inversion slice profiles. Only $M_z(z)$ is displayed. Note that the more ambitious the rate variation, the more smeared is the off-resonance slice profile. Finally, Fig. 17 shows an experimental spin-echo slice profile obtained with the minimum-SAR pulse described above and with the frequency synthesizer off resonance by 200 Hz.

IMPLEMENTATION DETAILS

Although the VERSE concept is essentially straightforward, there are a few implementation details sufficiently subtle to warrant explication. Since most imaging systems

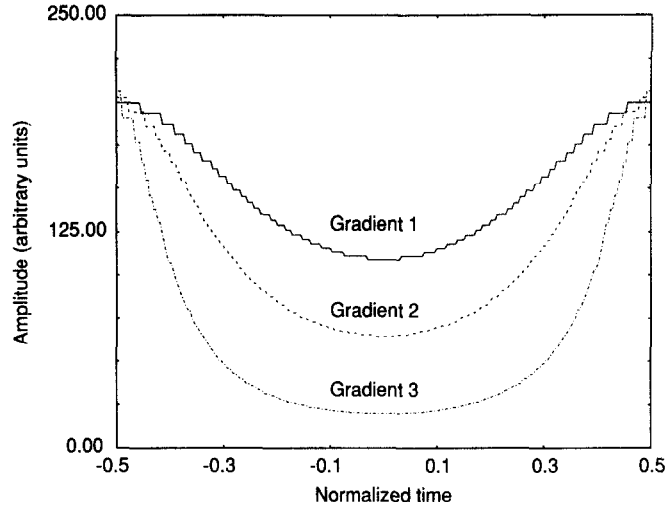

FIG. 15. Gradient waveforms showing degree of rate variation.

support only uniformly sampled waveforms, some form of interpolation of variable-rate pulses to a uniform-rate format is required. We also discuss a technique for limiting the gradient slew rate.

Interpolation. Implementing a variable-rate excitation waveform on an imaging system requires some interpolation to a uniformly sampled pulse. The problem then is to find uniform-rate pulses that have similar properties to the variable-rate waveforms. We have tried several techniques and discuss cubic spline interpolation and discrete rate variation.

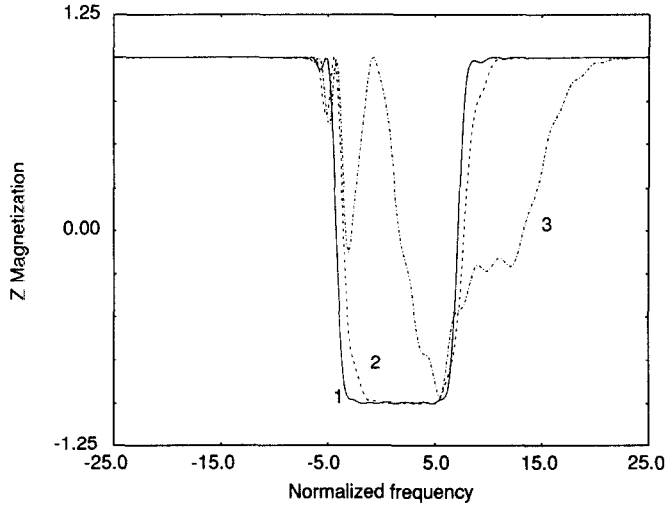

FIG. 16. $M_z(z)$ slice profiles off resonance by 200 Hz.

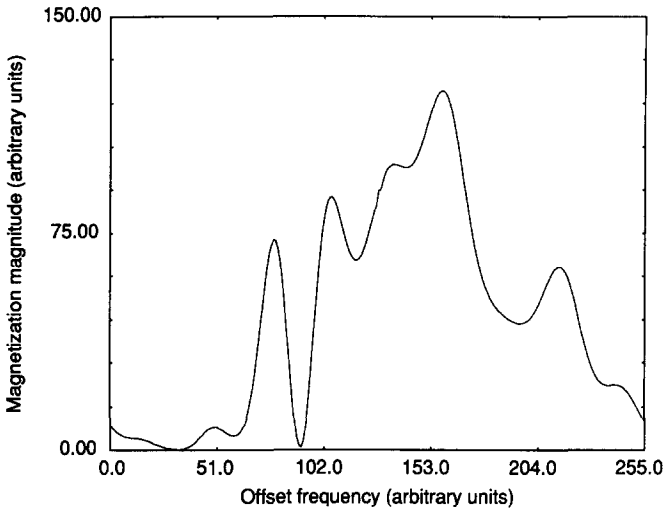

FIG. 17. Experimental minimum-SAR slice profile off resonance by 200 Hz.

Cubic spline interpolation (*9*) fits third-order polynomials through each of the ordered pairs $\{T(k), b_1(k)\}$, where $T(k)$ is the running sum of the individual $t(k)$:

$$T(k) = \sum_{i=1}^{k} t(i). \qquad [22]$$

The uniform-rate pulse is recovered by uniform sampling of the polynomials. This simple technique degrades the slice profile mildly; the degree of degradation depends on the smoothness of the variable-rate pulses and the number of samples in the uniform-rate pulse.

The technique of discrete rate variation is motivated by a desire to preserve slice fidelity. It is clear that one could obtain a uniform-rate pulse if the $t(k)$ were constrained to discrete values, say $n\Delta\tau$, by sampling this pulse at $\Delta\tau$. Moreover, the uniformly sampled pulse will excite an identical slice profile. This fact follows from the ordered product solution of the Bloch equation (*6*); one pulse of duration $n\Delta\tau$ may be replaced by n identical pulses of length $\Delta\tau$.

Note that the constraint to a discrete set of $t(k)$ will inherently limit the SAR reduction possible with VERSE, and that the smaller the τ the less the SAR penalty. An obvious drawback of this technique then is the inherent trade-off of flexibility for SAR reduction and the number of samples needed in the interpolated pulse. We have pursued a viable compromise by subsampling a very large array. This technique gives high-fidelity slice profiles with only 256 sample values.

Gradient waveform smoothing. A typical gradient slew-rate limitation is 2 G/cm/s. Both the minimum-SAR and minimum-time formulations produce gradient waveforms that violate this gradient constraint. We discuss here a simple smoothing algorithm that preserves the total duration of the pulse.

To avoid confusion over rising edge slope and falling edge slope, we define an average slew rate

$$\frac{\Delta g(i)}{\Delta t} \stackrel{\text{def}}{=} 2\,\frac{g(i+1)-g(i)}{t(i+1)+t(i)}. \qquad [23]$$

Geometrically, this represents the slope of the line joining the midpoints of two piecewise constant gradient pulses. Using the facsimile conditions,

$$\frac{\Delta g(i)}{\Delta t} = 2G\Delta t\,\frac{1/t(i+1)-1/t(i)}{t(i+1)+t(i)}. \qquad [24]$$

If the magnitude of the slew rate exceeds the maximum rate, then $t(i+1)$ and $t(i)$ can be altered to achieve the maximum slew rate while preserving the sum $t(i+1) + t(i)$. If we define $t_{\text{sum}} = t(i+1) + t(i)$ and the variable τ as the smoothed value of $t(i)$, then we need to solve the following equation for τ,

$$\alpha = \frac{1}{t_{\text{sum}}-\tau} - \frac{1}{\tau}, \qquad [25]$$

where

$$\alpha = \left(\frac{\Delta g}{\Delta t}\right)_{\max} \frac{t_{\text{sum}}}{2G\Delta t}. \qquad [26]$$

It is straightforward to show that

$$\tau = \frac{t_{\text{sum}}}{2} - \frac{1}{\alpha} \pm \sqrt{\frac{1}{\alpha^2} + \left(\frac{t_{\text{sum}}}{2}\right)^2}. \qquad [27]$$

The positive root must be taken when α is positive, that is, when the gradient slope is too steep. The negative root must be taken when α and, hence, the slope are negative. Since the duration of the gradient is preserved pairwise, the total duration is preserved. Of course, a new variable-rate RF pulse must be computed with the facsimile conditions from the smoothed gradient. We used this slew-rate limitation algorithm for all experimental results.

DISCUSSION

We have introduced the concept of variable-rate selective excitation and detailed an application to SAR reduction of selective pulses. Three algorithms for SAR and amplitude reduction were developed. The first offers the minimum-SAR facsimile pulse for a specified duration. The second finds the briefest pulse that does not exceed a specified peak-RF level. Finally, parametric gradients allow for constrained minimization of SAR with intrinsically smooth gradient waveforms. Experimental results for each algorithm were presented. Of the three algorithms, the parametric formulation offers the most robust SAR minimization, since these pulses seem to be the most forgiving of gradient-RF timing mismatches.

More experiments are required to determine the limitations of off-resonance slice degradation. It is possible that the natural chemical-shift slice degradation could be used to advantage when both spatial and chemical-shift selection are desired.

Although we have demonstrated VERSE only for 180° pulses and SAR-intensive

pulses, the technique is completely general. The emphasis was intended to illustrate that some excellent pulses with high SAR should now be reconsidered in a variable-rate format.

APPENDIX A. MINIMUM-SAR FACSIMILE

The minimum-SAR facsimile gradient design equation is

$$\min_{\mathbf{g}} \text{SAR}(\mathbf{g}) = \sum_{k=1}^{N} g(k)|B_1(k)|^2, \quad [28]$$

subject to maximum gradient and duration constraints:

$$g(k) < G_{\max}, \quad [29]$$

$$\sum_{k=1}^{N} \frac{1}{g(k)} = \frac{N}{G}. \quad [30]$$

Using Lagrange multipliers, we define the quantity $L(\mathbf{g}, \lambda, \mu)$;

$$L(\mathbf{g}, \lambda, \mu) = \sum_{k=1}^{N} l(g(k), \lambda, \mu_k), \quad [31]$$

where

$$l(g(k), \lambda, \mu_k) = g(k)|B_1(k)|^2 + \lambda\left[\frac{1}{g(k)} - \frac{1}{G}\right] + \mu_k(g(k) - G_{\max}). \quad [32]$$

The Lagrange multiplier λ is unspecified, but the components μ_k are restricted to be nonnegative (*10*). If one of the computed gradient values violates the $G_{\max}$ constraint, then the constraint is *active*. This implies that $g(k) = G_{\max}$ and $\mu_k > 0$. For *inactive* constraints, $\mu_k = 0$, and $g(k)$ is optimized as if it were unconstrained.

This is a separable problem and is best solved using dual methods. Following Luenberger (*10*), we solve for the quantity

$$\phi(\lambda, \mu) = \min_{\mathbf{g}} L(\mathbf{g}, \lambda, \mu). \quad [33]$$

Since the minimization is separable,

$$\phi(\lambda, \mu) = \sum_{k=1}^{N} \min_{g(k)} l(g(k), \lambda, \mu_k). \quad [34]$$

Minimizing over $g(k)$ yields

$$g(k) = \frac{\sqrt{\lambda}}{(|B_1(k)|^2 + \mu_k)^{1/2}}. \quad [35]$$

Note that for the inactive constraint case, $\mu_k = 0$ and

$$g(k) = \frac{\sqrt{\lambda}}{|B_1(k)|}. \quad [36]$$

This important result says that the $t(k)$ should be proportional to $|B_1(k)|$, so long as the G_{max} constraint is satisfied. Of course this means that the unconstrained optimal RF pulse has constant modulus, an intuitively appealing result. For the active case, we still need to optimize $\phi(\lambda, \mu)$ over λ and μ. Substituting $g(k)$ from Eq. [35] into $L(\mathbf{g}, \lambda, \mu)$ we obtain

$$\phi(\lambda, \mu) = \sum_{k=1}^{N} 2\sqrt{\lambda}(|B_1(k)|^2 + \mu_k)^{1/2} - \lambda/G - \mu_k G_{max}. \quad [37]$$

The derivative with respect to μ_k obtains

$$\frac{\sqrt{\lambda}}{(|B_1(k)|^2 + \mu_k)^{1/2}} = G_{max}. \quad [38]$$

Comparison with Eq. [35] verifies that the active $g(k)$ do indeed assume the value G_{max}. Hence,

$$g(k) = \min\left\{G_{max}, \frac{\sqrt{\lambda}}{|B_1(k)|}\right\}. \quad [39]$$

APPENDIX B. SHIFT THEOREM

SHIFT THEOREM. *If a pulse, $b_1(t)$, and gradient, $g(t)$, excite a slice* $\mathbf{M}(z, T)$, *then* $b_1(t)\exp\{iz_0\gamma \int_t^T g(\tau)d\tau\}$ *and the same gradient excite the slice* $\mathbf{M}(z - z_0, T)$.

Proof. Let $\tilde{b}(t) = b_1(t)e^{i\gamma z_0 \int_t^T g(\tau)d\tau}$. We define the profile $\mathbf{m}(z, T)$ to be the response to $\tilde{b}(t)$. We prove the theorem by showing that $\mathbf{m}(z, T) = \mathbf{M}(z - z_0, T)$. We assume that $\mathbf{M}(z, 0) = [0, 0, 1]^T$.

Neglecting relaxation, the Bloch equation for $\mathbf{m}(z, t)$ is

$$\frac{d\mathbf{m}(z, t)}{dt} = \gamma[\tilde{b}_I(t)\mathcal{X} + \tilde{b}_Q(t)\mathcal{Y} + g(t)z\mathcal{Z}]\mathbf{m}(z, t), \quad [40]$$

where the skew-symmetric basis matrices are

$$\mathcal{X} = \begin{bmatrix} 0 & 0 & 0 \\ 0 & 0 & 1 \\ 0 & -1 & 0 \end{bmatrix}, \quad \mathcal{Y} = \begin{bmatrix} 0 & 0 & -1 \\ 0 & 0 & 0 \\ 1 & 0 & 0 \end{bmatrix}, \quad \mathcal{Z} = \begin{bmatrix} 0 & 1 & 0 \\ -1 & 0 & 0 \\ 0 & 0 & 0 \end{bmatrix}.$$

The modulated pulse has the in-phase and quadrature components

$$\tilde{b}_I(t) = \cos\theta(t)b_I(t) - \sin\theta(t)b_Q(t), \quad [41]$$

$$\tilde{b}_Q(t) = \sin\theta(t)b_I(t) + \cos\theta(t)b_Q(t), \quad [42]$$

where we have defined $\theta(t) = \gamma z_0 \int_t^T g(\tau)d\tau$.

The proof relies on a spatially invariant change of coordinates:

$$\mathbf{P}(z, t) = e^{\mathcal{Z}\theta(t)}\mathbf{m}(z, t) \quad [43]$$

$$= \begin{bmatrix} \cos\theta(t) & \sin\theta(t) & 0 \\ -\sin\theta(t) & \cos\theta(t) & 0 \\ 0 & 0 & 1 \end{bmatrix}\mathbf{m}(z, t). \quad [44]$$

$\mathbf{P}(z, t)$ is the magnetization vector in a new "rotating frame." This frame rotates at a variable frequency, $-\gamma z_0 g(t)$. Note that the final slice profiles $\mathbf{P}(z, T)$ and $\mathbf{m}(z, T)$ are identical since $\theta(T) = 0$. Using the chain rule and some algebra, one can show that the Bloch equation for $\mathbf{P}(z, t)$ is

$$\frac{d\mathbf{P}(z, t)}{dt} = \gamma[b_1(t)\mathcal{X} + b_Q(t)\mathcal{Y} + g(t)(z - z_0)\mathcal{Z}]\mathbf{P}(z, t), \qquad [45]$$

where $b_1(t) = b_I(t) + ib_Q(t)$. This implies $\mathbf{P}(z, T) = \mathbf{M}(z - z_0, T)$. Since $\mathbf{P}(z, T) = \mathbf{m}(z, T)$, we conclude that $\mathbf{m}(z, T) = \mathbf{M}(z - z_0, T)$.

ACKNOWLEDGMENTS

The authors gratefully acknowledge the support of the General Electric Medical Systems Division, with special gratitude to Dr. Norbert Pelc and Ann Shimakawa for their invaluable help. This work was also supported by National Institutes of Health Contract HV-38045 and Grant HL-34962.

REFERENCES

1. A. LENT AND M. KRITZER, *in* "Proceedings, Fourth Annual Meeting of the Society for Magnetic Resonance in Medicine," August 1985, p. 1015.
2. S. M. CONOLLY, D. G. NISHIMURA, AND A. MACOVSKI, *IEEE Trans. "Medical Imaging"* **MI-5,** 106, (1986).
3. J. MURDOCH, A. LENT, AND M. KRITZER, *in* "Proceedings, Fifth Annual Meeting of the Society for Magnetic Resonance in Medicine," August 1986, p. 1434.
4. M. S. SILVER, R. I. JOSEPH, AND D. I. HOULT, *J. Magn. Reson.* **59,** 347, (1984).
5. O. COER-JOLY, L. DARRASSE, H. SAINT-JAMES, AND J. BITTOUN, *in* "Proceedings, Fifth Annual Meeting of the Society for Magnetic Resonance in Medicine," August 1986, p. 473.
6. P. MANSFIELD AND P. MORRIS, "NMR Imaging in Biomedicine," Academic Press, New York, 1982.
7. S. M. CONOLLY, D. G. NISHIMURA, AND A. MACOVSKI, *in* "Proceedings, Fifth Annual Meeting of the Society for Magnetic Resonance Imaging," February 1987, p. Mam–E4.
8. S. M. CONOLLY, D. G. NISHIMURA, AND A. MACOVSKI, *in* "Proceedings, Sixth Annual Meeting of the Society for Magnetic Resonance in Medicine," August 1987, p. 947.
9. G. E. FORSYTHE, M. A. MALCOLM, AND C. B. MOLER, "Computer Methods for Mathematical Computations," Prentice–Hall, Englewood Cliffs, New Jersey, 1977.
10. D. G. LUENBERGER, "Introduction To Linear and Nonlinear Programming," Addison–Wesley, Reading, Massachusetts, 1973.